ASTM INTERNATIONAL

Journal of Testing and Evaluation

Diego Ferreño,[1] David Fernández-Rucoba,[2] José A. Casado,[3] Roberto Bascones,[2] Estela Ruiz,[3] Álvaro Rodríguez,[2] Roberto Miguel,[4] and Enrique G. Poncela[4]

DOI: 10.1520/JTE20180569

Structural Integrity Assessment of a Nuclear Vessel through ASME and Master Curve Approaches Using Irradiation Embrittlement Predictions

Journal of Testing and Evaluation

doi:10.1520/JTE20180569 available online at www.astm.org

Diego Ferreño,[1] David Fernández-Rucoba,[2] José A. Casado,[3] Roberto Bascones,[2] Estela Ruiz,[3] Álvaro Rodríguez,[2] Roberto Miguel,[4] and Enrique G. Poncela[4]

Structural Integrity Assessment of a Nuclear Vessel through ASME and Master Curve Approaches Using Irradiation Embrittlement Predictions

Reference

Ferreño, D., Fernández-Rucoba, D., Casado, J. A., Bascones, R., Ruiz, E., Rodríguez, Álvaro, Miguel, R., and Poncela, E. G., "Structural Integrity Assessment of a Nuclear Vessel through ASME and Master Curve Approaches Using Irradiation Embrittlement Predictions," *Journal of Testing and Evaluation* https://doi.org/10.1520/JTE20180569.
ISSN 0090-3973

Manuscript received August 7, 2018; accepted for publication September 27, 2018; published online January 8, 2019.

[1] Laboratory of Science and Engineering of Materials, University of Cantabria, E.T.S. de Ingenieros de Caminos, Canales y Puertos, Av. Los Castros 44, Santander 39005, Spain (Corresponding author), e-mail: ferrenod@unican.es

[2] Technological Centre for Components, Parque Científico y Tecnológico de Cantabria C/ Isabel Torres n° 1, Santander 39011, Spain

[3] Laboratory of Science and Engineering of Materials, University of Cantabria, E.T.S. de Ingenieros de Caminos, Canales y Puertos, Av. Los Castros 44, Santander 39005, Spain

[4] Equipos Nucleares, S.A., S.M.E. Av. Juan Carlos I, 8, Maliaño 39600, Spain

ABSTRACT

The assessment of the structural integrity of nuclear vessels is based on a series of procedures developed in the 1970s and 1980s. On one hand, curves that, according to the American Society of Mechanical Engineers code, describe the relationship between steel toughness and temperature in the ductile-to-brittle transition region, based on the reference temperature concept RT_{NDT}, were adopted in 1972. On the other hand, the material embrittlement derived from the exposure of steel to neutron irradiation is determined through the model included in "Regulatory Guide 1.99 Rev. 2," published in 1988. Since then, there have been enormous advances in this field. For example, the Master Curve, based on the reference temperature T_0, describes the relationship between toughness and temperature in the transition zone more realistically and with much more robust microstructural and mechanical foundations and uses the elastic-plastic fracture toughness K_{Jc}. Moreover, improved models have been developed to estimate the embrittlement of steel subjected to neutron irradiation, such as ASTM E900, *Standard Guide for Predicting Radiation-Induced Transition Temperature Shift in Reactor Vessel Materials*. This study is aimed at comparing the results obtained using traditional procedures to the improved alternatives developed later. For this purpose, the behavior of the steel of a nuclear vessel that is currently under construction has been experimentally characterized through RT_{NDT} and T_0 parameters. In addition, the material embrittlement has been quantified using "Regulatory Guide 1.99 Rev. 2" and ASTM E900. These experimental results have been transferred to the assessment of the structural integrity of the vessel to determine

the pressure-temperature limit curves and size of the maximum admissible defect as a function of the operation time of the plant. The results have allowed the implicit overconservatism present in the traditional procedures to be quantified.

Keywords

nuclear vessel, ductile-to-brittle transition region, neutron embrittlement, Master Curve, structural integrity

Introduction

Neutron irradiation is the most relevant source of degradation for nuclear reactor pressure vessel (RPV) steels. Because of the irradiation, the material fracture toughness decreases over time, leading to a shift in the ductile-to-brittle transition (DBT) temperature. The surveillance program of the plant makes it possible to monitor changes in the fracture toughness of the vessel steel; from this information, the conditions under which the vessel can be operated throughout its in-service life can be determined. A surveillance program consists of placing capsules holding specimens fabricated with the same steel as that of the vessel in the beltline region (that is, the general area of the reactor vessel near the core midplane where radiation dose rates are at their highest) and attaching them to the inside wall of the vessel. Thus, the specimen irradiation history duplicates the neutron spectrum, temperature history, and maximum neutron fluence undergone by the reactor vessel's inner surface.

The fracture toughness requirements for ferritic materials of nuclear power plants (NPPs) must fulfill the acceptance and performance criteria of Appendix G of Section III of the American Society of Mechanical Engineers (ASME) *Boiler and Pressure Vessel Code* [1,2]. According to this procedure, the fracture resistance of the vessel material in the DBT region before irradiation is described by the reference temperature $RT_{NDT(U)}$, which is obtained from Charpy impact and Pellini drop weight tests through empirical and conservative correlations. The Master Curve (MC) is an alternative method based on direct characterization of the fracture toughness in the DBT region by means of K_{Jc} tests. This approach is a consequence of the developments in elastic-plastic fracture mechanics (EPFM) together with an increased understanding of the micromechanisms of cleavage fracture. The basic MC method for analysis of brittle fracture test results is defined in ASTM E1921-17a, *Standard Test Method for Determination of Reference Temperature, T_0, for Ferritic Steels in the Transition Range* (Superseded) [3], where the reference temperature T_0 is employed. T_0 is defined as the temperature at which the median fracture toughness obtained with $B = 25.4$ mm thickness (1T, according to ASTM terminology) specimens is 100 MPa $\cdot$ m$^{1/2}$. The reference temperature T_0 completely characterizes the fracture toughness in the DBT region of ferritic steels that experience an onset of cleavage cracking at elastic or elastic-plastic K_{Jc} instabilities. This fact is well supported by experience.

The predictions of these approaches (ASME and MC) have been compared in this study for the vessel steel of a boiling water reactor that is currently under construction. Thus, to quantify the level of inherent conservatism, two approaches have been compared in this work. First, Pressure-Temperature limit curves (P-T curves) have been obtained following the ASME code that consistently incorporates the MC approach. These curves relate the maximum allowable pressure with the operation temperature in order to avoid any risk of brittle fracture of the vessel for a postulated flaw with a depth equal to one quarter of the thickness of the vessel ($t/4$). Second, the allowable crack size has been calculated for the heat-up and cooldown operations as well as the hydrostatic test of the vessel. In this latter case, the stress intensity factors have been obtained by means of ASME Code Section XI [2] as well as the European Fitness-for-Service Network (FITNET) Fitness-for-Service (FFS) procedure [4]. To achieve these goals, the fracture properties of the unirradiated base metal of the vessel in the DBT region were experimentally obtained. In this sense, Charpy and Pellini tests were carried out to apply the ASME code, whereas K_{Jc} fracture toughness tests were performed to apply the FITNET FFS procedure. Furthermore, the fracture properties of the irradiated material were predicted by using a series of analytical models available in standards and literature. Then, an assessment of structural integrity was also carried out for the irradiated condition based on these models for neutron embrittlement.

Materials and Methods

REGULATORY METHOD REGARDING FRACTURE TOUGHNESS IN THE DBT REGION

Title 10 of the *Code of Federal Regulations*, 10CFR50 [5], imposes P-T limits on the reactor coolant pressure boundary for NPPs designed in the USA. According to this law, fracture toughness of ferritic materials must fulfill the acceptance and performance criteria of Appendix G of Section III of the ASME *Boiler and Pressure Vessel Code* [1]. The toughness of the vessel steel in the DBT region before irradiation is described by means of the reference temperature $RT_{NDT(U)}$, which is obtained through the combination of Charpy impact and Pellini drop weight tests. This parameter is used to index two generic curves [1,2] relating toughness versus temperature (see Eqs 1 and 2, in which temperatures must be expressed in °C and toughness is obtained in MPa · $m^{1/2}$). The K_{Ic} curve describes the lower envelope to a large set of K_{Ic} data, while the K_{IR} is a lower envelope to a combined set of K_{Ic}, K_{Id} (dynamical tests), and K_{Ia} (crack arrest tests) data, therefore being more conservative than the former. This approach is based on Linear Elastic Fracture Mechanics (LEFM) and assumes that the ASME curves are representative of a wide variety of vessel steels; large scatter, typical in the DBT region, is avoided by taking lower envelopes into account. Consequently, the method provides a deterministic and excessively conservative response in most cases.

$$K_{Ic} = 36.45 + 22.766 \cdot e^{0.036 \cdot (T - RT_{NDT})} \tag{1}$$

$$K_{IR} = 29.40 + 13.675 \cdot e^{0.0261 \cdot (T - RT_{NDT})} \tag{2}$$

THE MC

The MC approach was originally proposed by Wallin [6–9] to statistically describe the fracture toughness in the DBT region and is based on the experimental characterization of the fracture toughness. This method is a consequence of the developments in EPFM together with an increased understanding of the micromechanisms involved in cleavage fracture. The basic MC method for analysis of brittle fracture test results is defined in ASTM E1921-17a [3]. The mathematical and empirical details of the procedure are available in Ref. [10]. Some examples of successful applications can be found in Refs. [11–16]. The main features and advantages of the method are hereafter summarized:

- Fracture is governed by the weakest link statistics, which follows a three-parameter Weibull distribution. One of the main advantages of the method is that it allows data from different-sized specimens to be compared. As thickness increases, the material toughness K_{Jc} is reduced, which is due to the higher probability of finding a critical particle for the applied load. ASTM E1921-17a [3] provides Eq 3 to relate the fracture toughness, K_{Jc}, for specimens of different thickness.

$$K_{Jc,2} = K_{min} + (K_{Jc,1} - K_{min}) \cdot \left(\frac{B_2}{B_1}\right)^{\frac{1}{4}} \tag{3}$$

- Eq 4 provides the value of K_{Jc} for a given cumulative failure probability, P_f, once T_0, the so-called MC reference temperature, has been determined. T_0 corresponds to the temperature such that the median fracture toughness for a 25.4-mm-thick specimen (1T) has the value 100 MPa · $m^{1/2}$. The confidence bounds of the distribution (usually taking $P_f = 0.01$ or 0.05 for the lower bound and 0.95 or 0.99 for the upper bound) can be obtained by applying Eq 4. As a particular case, the expression for the median fracture toughness ($P_f = 0.5$) is determined as seen in Eq 5.

$$K_{J_c,P_f} = K_{min} + \left[-ln(1 - P_f)\right]^{0.25} \cdot \left[11 + 77 \cdot e^{0.019 \cdot (T - T_0)}\right] \tag{4}$$

$$K_{J_c(med)} = 30 + 70 \cdot e^{0.019 \cdot (T - T_0)} \tag{5}$$

- A fitting procedure must be applied to find the optimum value of T_0 for a particular set of experimental data (K_{Jc} and test temperature). For this task, all data are thickness-adjusted to the reference specimen thickness $B_0 = 25.4$ mm (1T) using Eq 3. The procedure can be applied either to a single test temperature or transition curve data. In the latter approach, T_0 is estimated from the size-adjusted K_{JC} data ($K_{JC,1T}$) using a multi-temperature maximum likelihood method.
- This statistical analysis to estimate T_0 can be reliably performed even with a small number of fracture toughness tests (usually between six and ten specimens). Moreover, as an EPFM approach is used, the specimen size requirements are much less demanding than those of LEFM [17]. These remarks are of great relevance for nuclear reactor surveillance programs for which the amount of material available is usually very limited and consists of small-size samples (Charpy V-notch (CVN) specimens).
- To estimate the reference temperature T_0, a previous censoring of the non-size-adjusted data must be applied. Fracture toughness data that are larger than the validity limit given by Eq 6, as defined in Ref. [3], are reduced to the validity limit, $K_{Jc(lim)}$, and treated as censored values in the subsequent estimation stage. This condition is imposed to guarantee high constraint conditions in the crack front during the fracture process.

$$K_{J_{c(lim)}} = \sqrt{\frac{E \cdot s_Y \cdot b_0}{30 \cdot (1-\nu^2)}} \tag{6}$$

where s_y is the yield stress at the test temperature, E is the Young's modulus, b_0 is the initial ligament, and ν is Poisson's ratio ($\nu = 0.3$ in this case). It must be stressed that the factor of 30 in Eq 6 is currently under discussion [10] and that, for instance, ASTM E1820-17, *Standard Test Method for Measurement of Fracture Toughness* (Superseded) [18], imposes a more demanding limit with a factor of 50 or 100, depending on the nature of the steel.

- The standard deviation in the estimate of T_0, expressed in °C, is given by Eq 7:

$$\sigma_{T_0} = \frac{\beta}{\sqrt{r}} \tag{7}$$

where r represents the total number of valid specimens (uncensored results) used to establish T_0. The values of factor β are provided in Ref. [3].

- As stated in Ref. [3], the reference temperature T_0 must be determined from quasistatic strain rates. However, the experimental evidence shows that the MC concept can also be applied to dynamic tests [13,14,19–21]. In this sense, Wallin [19] has proposed a simple semiempirical expression for the strain rate dependence of T_0. The error of the expression is only about ±20 %, covering yield strengths from 200 to 1,000 MPa.

CORRELATIONS TO PREDICT THE MATERIAL EMBRITTLEMENT

The decrease in material toughness that is due to neutron irradiation in the DBT region is currently estimated through empirical methods based on the shift undergone by Charpy impact curves that are obtained from the surveillance capsule specimens, which are retrieved periodically according to the plant withdrawal schedule. As stated in 10CFR50 [5], the effect of neutron fluence on the behavior of the material is predicted by "Regulatory Guide 1.99 Rev. 2" [22], which provides Eq 8 for the evolution of RT_{NDT}:

$$RT_{NDT} = RT_{NDT(U)} + \Delta RT_{NDT} + M \tag{8}$$

where ΔRT_{NDT} represents the shift in the reference temperature that is due to irradiation (which is assumed to be equal to the shift of the Charpy transition curve indexed at 41 J; thus, $\Delta RT_{NDT} = \Delta T_{41\,J}$). The third term, M, is the margin that must be added to obtain a conservative estimation. The procedure in Ref. [22] enables ΔRT_{NDT} to be obtained even when no credible surveillance data are available by means of an equation based on the chemistry of the steel (copper and nickel content) and the neutron fluence received.

Moreover, in 2002, the ASTM committee approved ASTM E900-15e1, *Standard Guide for Predicting Radiation-Induced Transition Temperature Shift in Reactor Vessel Materials* [23], to predict the radiation-induced transition temperature shift (TTS) in reactor vessel materials. The embrittlement correlation proposed, which allows ΔT_{41J} to be estimated, is based on the copper and nickel content, irradiation temperature, and neutron fluence. The expression is mechanistically guided based on the current understanding of two mechanisms of embrittlement, stable matrix damage (SMD) and copper-rich precipitation (CRP). Saturation of copper effects (for different weld materials) was included. The mean value of the TTS is based on adding these two contributions, as stated in Eq 9:

$$\mathrm{TTS} = \mathrm{SMD} + \mathrm{CRP} \tag{9}$$

Several important features of the model are summarized as follows:

- The SMD contribution depends on the irradiation temperature and neutron fluence.
- The CRP term is dependent on the copper and nickel content and neutron fluence, including a specific material factor (which distinguishes between weld, forgings, etc.). When the copper content is less than 0.072 wt. %, then CRP = 0, and the maximum copper content considered is 0.305 wt. % for welds.
- The standard error of the correlation is 22.0°F (12.2°C).
- The neutron fluence rate is not included in the model. Although the surveillance capsule database includes neutron fluence rates ranging from $2 \cdot 10^8$ n/cm^2/s to $1 \cdot 10^{12}$ n/cm^2/s, the preponderance of the data lies between $3 \cdot 10^9$ n/cm^2/s and $2 \cdot 10^{11}$ n/cm^2/s. Within the limitations of the surveillance capsule database, a neutron fluence rate effect could not be unambiguously identified.

As a final remark, it is generally accepted that an approximate 1:1 correlation (slightly different for base and weld metals) does exist between the irradiation-induced shifts ΔRT_{NDT} and ΔT_0, as illustrated by an international database compiled by Sokolov and Nanstad from various publications [24]. In this sense, the linear fitting $\Delta T_0 = 1.04 \cdot \Delta T_{41\ \mathrm{J}}$ is proposed (for a database of 126 data points, including both base and weld materials) with an uncertainty of 34°C.

AVAILABLE MATERIAL

The specimens and samples tested in this study were obtained from the base material of the surveillance semiring of an actual nuclear vessel that was recently manufactured (the plant is currently under construction). The surveillance ring was extracted from one of the forged rings that were subsequently welded to manufacture the beltline of the RPV. The base material is carbon steel grade SA-508M Grade 3 Class 1 by ASME Section II [25]. This steel was subjected to normalizing-tempering plus quenching-tempering heat treatment after forging. The specimens employed in this study were selected to determine all the material parameters needed to conduct the structural integrity assessments (ASME versus MC). Specifically, the following tests were carried out: chemical composition tests, tension tests (as a function of temperature), Charpy impact tests (as a function of temperature), Pellini Drop-Weight (DW) tests, and K_{Jc} fracture toughness tests (to determine the reference temperature T_0); moreover, the fracture surfaces were examined by means of Scanning Electron Microscopy (SEM). These experimental methods are described in the sections "Available Material" through "Fracture Toughness Tests" in "Materials and Methods." Following the recommendation of Ref. [26], the samples were obtained at depths of 1/4 and 3/4 of the thickness of the ring. **Fig. 1** shows the distribution of specimens in the semiring; note that tension specimens were obtained in L and T orientations and Charpy specimens were obtained in LT and TL orientations. **Table 1** summarizes the number and purpose of the specimens employed in this study.

CHEMICAL COMPOSITION

The chemistry of the steel was determined using X-ray fluorescence spectrometry by means of an ARL QUANTRIS Optical Emission Spectrometer (Thermo Fisher Scientific, Waltham, MA).

FIG. 1 Distribution of specimens in the sector of the surveillance ring used in this study.

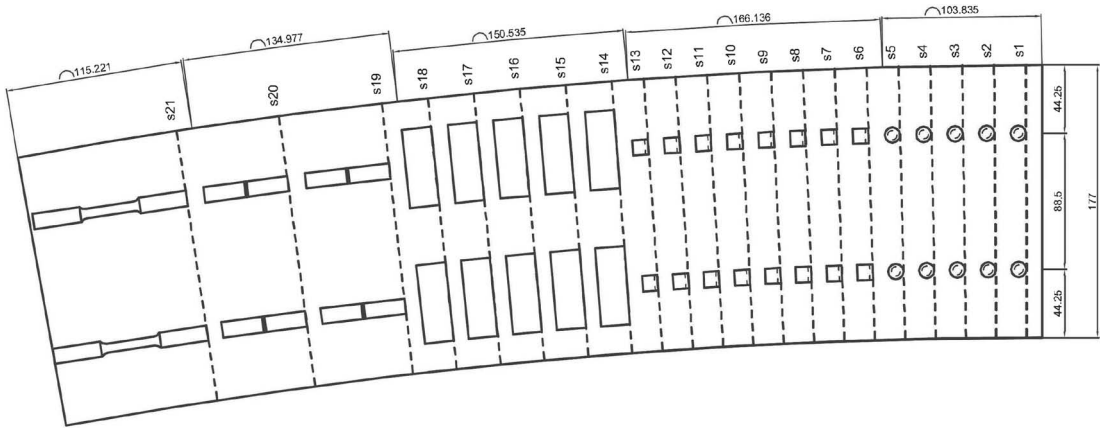

TABLE 1
Description of the experimental scope.

Specimen Type	Orientation	Number	Objectives
CVN Charpy	TL	12	Characterization of the Charpy toughness in the DBT region
	LT	12	in the LT and TL orientations.
	TL	15	Characterization of the K_{Jc} toughness in the DBT region in the LT and
	LT	15	TL orientations to determine T_0.
	TL	5	Reserved specimens.
	LT	5	
Tension	T	10	Determination of the tensile properties in the L and T orientations for a wide
	L	10	range of temperatures (from −145°C to 300°C).
Pellini DW	–	10	Attainment of the NDT.

TENSION TESTS

Tensile properties are necessary to evaluate the maximum measurement capacity in K_{JC} fracture toughness tests, as seen in ASTM E1921-17a [3]; see Eq 7. Ten tension tests were carried out for each of the orientations at temperatures ranging from −145°C to 300°C by means of an Instron 8501 universal testing machine (Norwood, MA) at a fixed strain rate of 10^{-3} min^{-1}. The tension tests were carried out according to ASTM E8 / E8M-16a, *Standard Test Methods for Tension Testing of Metallic Materials* [27]. The load-elongation curves were recorded up to fracture by using extensometers designed to operate at low and high temperatures.

CHARPY IMPACT TESTS

The CVN impact tests were performed and analyzed according to ASTM E23-16b, *Standard Test Methods for Notched Bar Impact Testing of Metallic Materials* [28]. Tests were carried out by means of an AMSLER RKP 300 (Zamudio, Spain) device with a loading capacity of 300 J.

PELLINI DW TESTS

The DW tests were performed following the requirements of ASTM E208-06(2012), *Standard Test Method for Conducting Drop-Weight Test to Determine Nil-Ductility Transition Temperature of Ferritic Steels* (Superseded) [29]. The test machine, which was designed and manufactured in agreement with Ref. [29], is shown in Fig. 2.

FIG. 2

Pellini DW test machine.

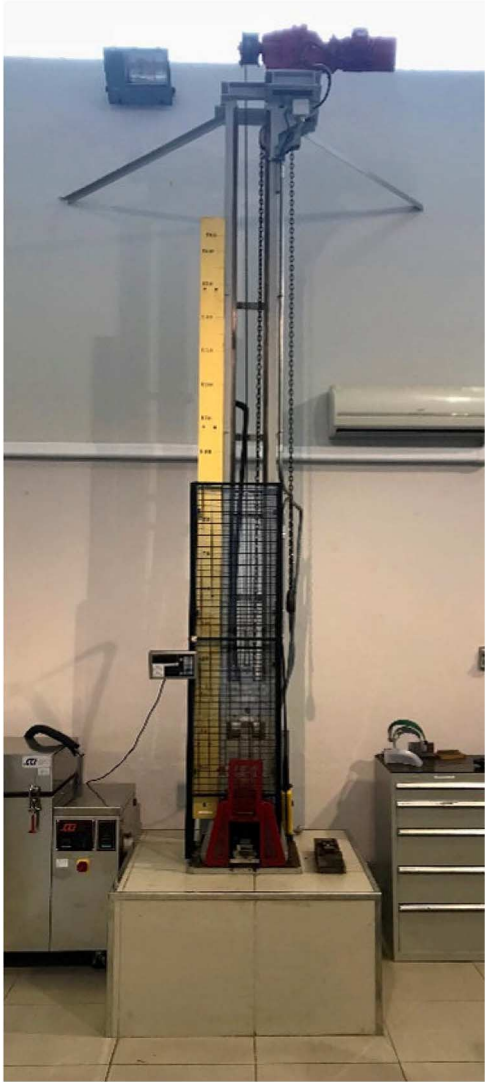

FRACTURE TOUGHNESS TESTS

The fracture K_{Jc} tests were carried out on single-edge notched bending SEN(B) specimens according to ASTM E1921-17a [3] (which also enables the use of compact tension (CT) or disk-shaped specimens). The fatigue precrack was produced at room temperature using the tensile properties of the steel (previously obtained) to choose the fatigue loads. The standard [3] requires the relation between the initial fatigue crack length and the width of the specimen, a_0/W, to be within the interval of 0.45–0.55. This requirement has been fully satisfied in all cases.

The fracture test temperatures were selected using the empirical correlations provided in Ref. [3], based on the values of $T_{28\ \mathrm{J}}$ and $T_{41\ \mathrm{J}}$ (determined from the Charpy tests). It is worth noting that these are only indicative correlations and may be inaccurate; nevertheless, the multitemperature procedure permits different specimens to be tested at different temperatures, getting closer to T_0 as the number of tests increases. The test temperatures ranged from −120°C to −82°C.

The loading method consisted of applying a controlled rate of crack opening displacement as measured at the load line (0.06 mm/min ~ 0.38 MPa · $m^{1/2}$ · s^{-1}). The J-integral was calculated from the load-crack opening displacement curve at crack instability, in accordance with the ASTM standard [3].

SEM FRACTOGRAPHIC STUDY

The fracture surfaces of the K_{Jc} tests were examined by SEM to ascertain the existence of cleavage as the physical fracture mechanism and to localize the initiation sites. The SEM device EVO MA 15 (Zeiss, Oberkochen, Germany) was employed.

Results

CHEMICAL COMPOSITION

Table 2 shows the chemical composition of the vessel as well as the ranges and limits imposed by the specifications [25]. A total of four chemical analyses were performed; then, the mean μ and standard deviation σ for each of the elements were obtained, as shown in Table 2. The main goal of these analyses is to determine the amount of those chemical elements that enhances the irradiation embrittlement, such as copper and nickel, in order to obtain the shift in DBT according to the models introduced in the "Correlations to Predict the Material Embrittlement" section. Note that the limits imposed by Section II of the ASME Code [25] for SA-508M Grade 3 Class 1 are satisfied in all cases.

TENSION TESTS

Fig. 3 shows the experimental results, yield stress, and tensile strength of the tension tests carried out in L (Fig. 3a) and T (Fig. 3b) orientations. The temperature dependence of the yield stress s_Y and ultimate strength s_U were fitted using suitable expressions of the form $s = C_0 + C_1 \cdot \exp(-C_2 \cdot T)$ (where C_0, C_1, and C_2 are the fitting parameters). The results of the fittings are compiled in Table 3.

The data fittings are included in the figure. Knowledge of the tensile properties is necessary to evaluate the maximum measurement capacity, as seen in ASTM E1921-17a [3]; see Eq 8. As can be observed, the material response is highly isotropic since there are no significant differences between the L and T orientations.

CHARPY IMPACT TESTS

The results of the Charpy tests are represented in Fig. 4. The energy absorbed, E, is shown in Fig. 4a, in which the dashed lines represent relevant energy levels (27 J, 41 J, and 68 J) to define the DBT (e. g, $T_{28\ J}$, $T_{41\ J}$, and $T_{68\ J}$,

TABLE 2

Chemical composition (wt. %) of the steel (mean and standard deviation) and comparison with the limits of the ASME Code [25].

Element	Measure 1	Measure 2	Measure 3	Measure 4	μ	σ	ASME Section II
C	0.20	0.19	0.19	0.18	0.190	0.008	≤0.25
Si	0.19	0.18	0.18	0.18	0.183	0.005	≤0.40
Mn	1.43	1.41	1.41	1.42	1.42	0.01	1.20–1.50
P	<0.012	<0.012	<0.012	<0.012	<0.012	–	≤0.025
S	<0.012	<0.012	<0.012	<0.012	<0.012	–	≤0.025
Ni	0.85	0.84	0.84	0.84	0.843	0.005	0.40–1.00
Cr	0.10	0.10	0.10	0.10	0.10	0	≤0.25
Mo	0.53	0.53	0.53	0.54	0.533	0.005	0.45–0.60
V	<0.02	<0.02	<0.02	<0.02	<0.02	–	≤0.05
Cu	<0.06	<0.06	<0.06	<0.06	<0.06	–	≤0.20
Ti	<0.022	<0.022	<0.022	<0.022	<0.022	–	≤0.015
Al	0.02	0.02	0.02	0.02	0.02	0	≤0.025

FIG. 3 Influence of temperature on yield stress and tensile strength: (a) L orientation and (b) T orientation.

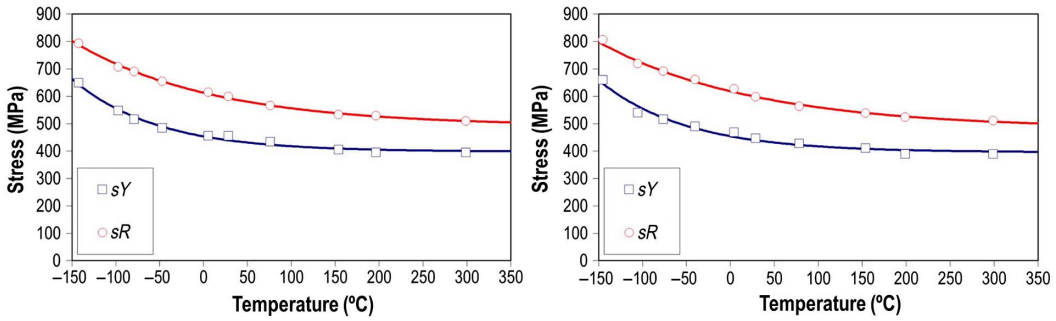

TABLE 3

Parameters of the exponential fitting of the stress-temperature curves.

	Orientation L			Orientation T		
	$s_{Y,max}$	$s_{Y,min}$	s_R	$s_{Y,max}$	$s_{Y,min}$	s_R
C_0	404.3	398.0	491.2	395.7	395.7	481.3
C_1	54.72	55.88	121.7	49.87	58.71	137.2
C_2	0.01142	0.01039	0.00626	0.01197	0.01000	0.00558

FIG. 4 Results of the CVN tests in the LT and TL orientations: (a) absorbed energy versus temperature, (b) *LE* versus temperature, and (c) *SFA* versus temperature.

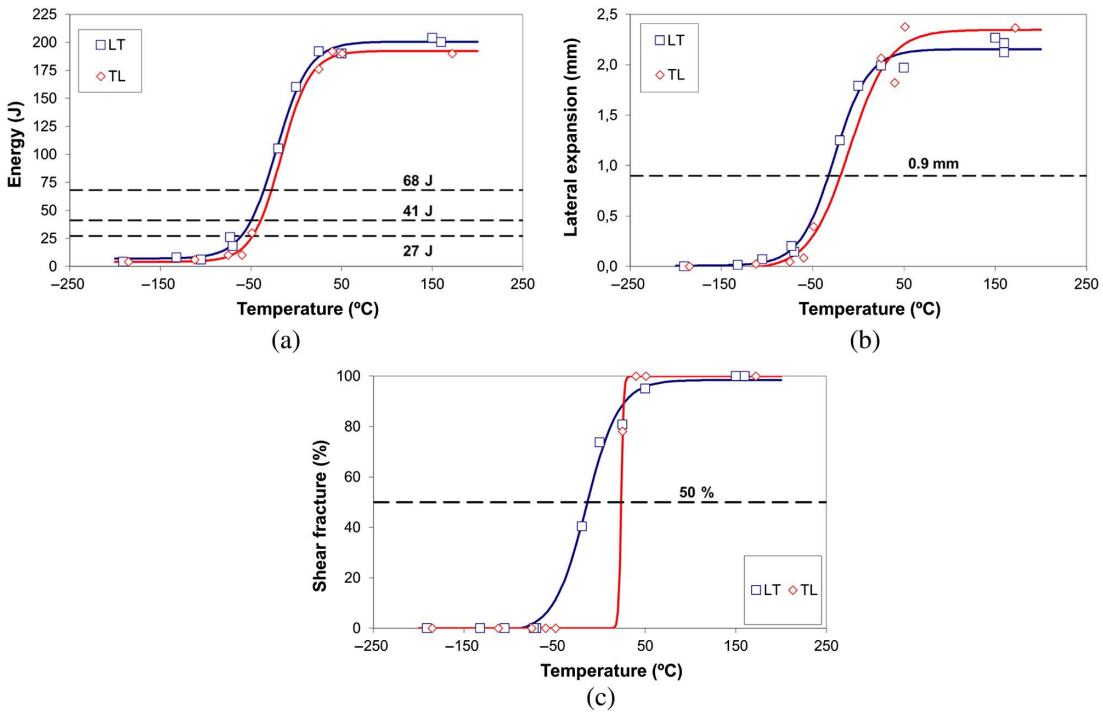

TABLE 4
Relevant results derived from the CVN impact test.

	LT	TL
$T_{27\ J}$, °C	−60.8	−48.3
$T_{41\ J}$, °C	−49.8	−39.3
$T_{68\ J}$, °C	−36.0	−27.4
USE, J	200.6	192.3
LSE, J	7.0	4.1
$T_{0.9\ mm}$, °C	−32.5	−19.5
$T_{50\ \%}$, °C	−13.8	23.4

respectively). In Fig. 4b, the lateral expansion, LE, is represented against temperature; the dashed line corresponds to $LE = 0.9$ mm. Finally, in Fig. 4c, the shear fracture appearance, *SFA*, is plotted against temperature; $SFA = 50$ % is represented by means of a horizontal line. The experimental data were fitted by means of hyperbolic tangent curves of the form E (or LE) $= A + B \cdot \tanh[(T - C)/D]$. These fittings were used to obtain a number of relevant results for LT and TL orientations that are summarized in Table 4, including the values of upper shelf energy (USE), lower shelf energy (LSE) as well as some representative transition temperatures (such as $T_{27\ J}$ and $T_{41\ J}$, among others).

As can be seen, the fracture behavior in LT and TL orientations is very similar. The only discrepancy is observed in $T_{50\ \%}$ (Table 4). However, this result should be interpreted as an artifact derived from the fitting of the data, as can be clearly appreciated in Fig. 4c.

PELLINI DW TESTS

The Pellini DW test provides the Nil-Ductility Temperature (NDT). The experimental results obtained in this study are shown in Table 5. RT_{NDT} is the material/heat-specific transition temperature defined by ASME Code Section III [1], Subsection NB-2300; it is based on a combination of the DW NDT and results from the CVN tests. According to the standard, the temperature NDT = 33.3°C = 13.3°C must be compared with T_{68J} (=−27.4°C) and $T_{0.9\ mm}$ (=−19.5°C) for the weakest material orientation (TL). Considering these values, it is concluded that RT_{NDT} = NDT = −20°C.

FRACTURE TOUGHNESS TESTS

In Fig. 5, the experimental results of K_{Jc} toughness for LT (Fig. 5a) and TL (Fig. 5b) material orientations are represented as a function of the test temperature T. The reference temperatures T_0 are indicated in the figure ($T_0 = -103.04$°C and −97.05°C for the LT and TL orientations, respectively) as well as several confidence bands (0.99, 0.95, 0.5, 0.05, and 0.01). The red points represent censored data (Eq 6) according to ASTM E1921-17a [3]. This standard enables the uncertainty in T_0, ΔT_0, to be determined; in this case, ΔT_0 is 5.4°C for LT and 6.0°C for TL orientations.

Additionally, the test procedure requires the crack length to be measured for each specimen once the test is completed (provided that an unstable brittle fracture occurred). The measurement for crack length

TABLE 5
Experimental results obtained from the Pellini DW test.

Specimen	Type	Temperature, °C	Result	NDT
P1	P2	−35	Break	–
P2	P2	−30	Break	–
P3	P2	−20	Break	−20°C
P4	P2	−15	No Break	–
P5	P2	−15	No Break	–

FIG. 5 K_{JC} versus temperature for (a) LT and (b) TL orientations. Confidence bounds of 0.99, 0.95, 0.5 (median), 0.05, and 0.01 are included.

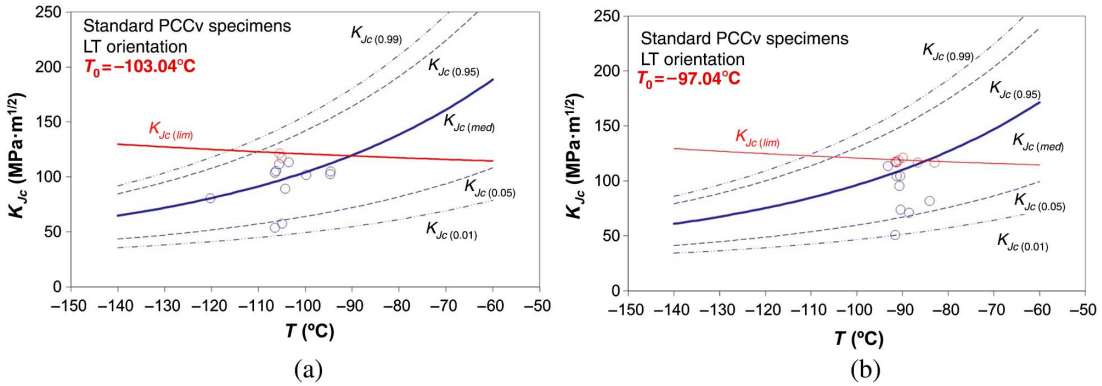

FIG. 6 (a) Measurement of the crack length in a PCCv standard specimen and (b) fractography showing the crack front after precracking and the region of brittle fracture, dominated by cleavage micromechanisms.

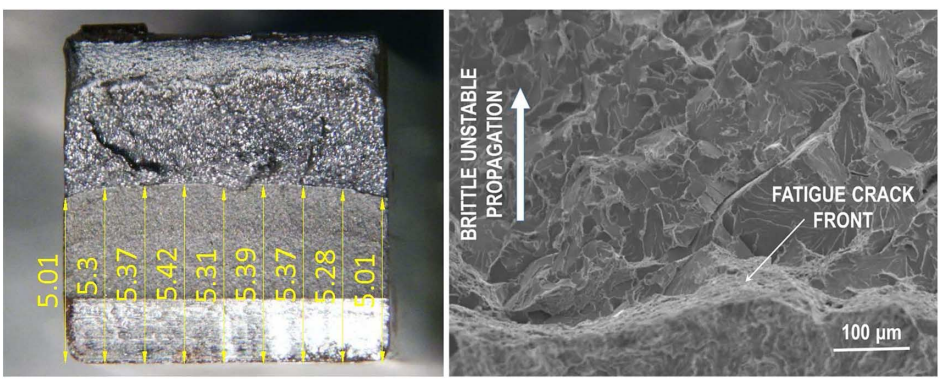

in precracked Charpy V-notch (PCCv) specimens is shown in Fig. 6a. Moreover, according to ASTM E1921-17a [3], "T_0 characterizes the fracture toughness of ferritic steels that experience onset of cleavage cracking…" and "For any test terminated with no cleavage fracture…the test record is judged to be a nontest, the result of which shall be discarded." For this reason, all fracture surfaces have been examined by means of SEM. Fig. 6b shows a picture in which the border between the fatigue precrack and the region of unstable propagation can be seen. Cleavage was the fracture micromechanism in this region, as demanded by the standard.

In this study, T_0 values were obtained through SEN(B) specimens. As stated in ASTM E1921-17a [3], "there is an expected bias among T_0 values as a function of the standard specimen type […]. On average, T_0 values obtained from CT specimens are higher than T_0 values obtained from SE(B) specimens. Best estimate comparison indicates that the average difference between CT and SE(B)-derived T_0 values is approximately 10°C." In this sense, it is important to follow the following recommendation, as given by the standard: "It is therefore strongly recommended that the specimen type be reported along with the derived T_0 value in all reporting, analysis, and discussion of results."

Structural Analysis

The P-T limit curves and maximum allowable crack length were the two elements selected to assess the structural integrity of the vessel and determine the influence of different analytical methods. All calculations were coded in MATLAB (MathWorks, Natick, MA). The most notable characteristics are summarized as follows:

- Calculations were carried out considering the unirradiated material condition as well as three representative levels of irradiation: 20, 40, and 60 Effective Full Power Years (EFPY), respectively. According to the design parameters of the nuclear plant, the expected neutron fluences for these exposure times are $6.9E+18$, $1.38E+19$, and $2.07E+19$ n/cm^2. The irradiation embrittlement of the vessel ($\Delta T_{41\ J}$, ΔT_0) was obtained using the predictive methods provided by "Regulatory Guide 1.99 Rev. 2" [22] and ASTM E900-15e1 [23].
- When considering irradiation embrittlement, the attenuation of neutron fluence through the thickness of the vessel was modeled by applying the exponential formula provided by "Regulatory Guide 1.99 Rev. 2" for that purpose.
- The three methods introduced in the "Regulatory Method Regarding Fracture Toughness in the DBT region" and "The MC" sections to describe the relationship between fracture toughness and temperature in the DBT region were implemented. The regulation in force (Appendix G of 10CFR50 [5]) is based on the ASME Code (Section XI, Appendixes A and G [2]), which establishes Curves (1) or (2) to be used (Curves K_{Ic} and K_{IR}). On the other hand, an alternative method based on the MC description of the DBT region (ASTM E1921-17a [3]) was used. Without loss of generality, a failure probability $P_f = 0.05$ was imposed for all the calculations based on the MC method.
- The ASME Code Section XI [2] imposes a postulated crack with a depth of $a = t/4$, t being the thickness of the vessel ($t = 177$ mm in this case). In addition, the following four different crack orientations may be considered:
- Inside or outside surface axially oriented defect (the plane of the crack is perpendicular to the hoop stress in the cylinder, σ_θ).
- Inside or outside surface circumferentially oriented defect (the plane of the crack is perpendicular to the axial stress in the cylinder, σ_z).
- Note that the hoop stress is higher than the axial stress ($\sigma_\theta > \sigma_z$); indeed, for a thin-walled cylinder, $\sigma_\theta = 2 \cdot \sigma_z$.
- 10CFR50 Appendix G [5] considers the following two scenarios for structural assessments: (i) hydrostatic pressure test (preservice or in-service), (ii) transient thermal conditions (heating-up and cooling-down operations of the vessel). The heating-up and cooling-down rate was 100°F/h, and critical core was considered in both cases (which is the most demanding situation under normal operations).
- Calculations were carried out by applying LEFM, according to which brittle fracture occurs when the stress intensity factor K_I reaches material fracture toughness (K_{Ic} or K_{IR}, depending on whether Curve (1) or (2) is used (see Refs. [1,2]), or K_{Jc} if the MC approach is used). The following failure condition must be applied to obtain the P-T curves:

$$SF \cdot K_{IM} + K_{It} \leq Toughness \tag{10}$$

  where SF is the safety factor (1.5 and 1.1 for the preservice and in-service hydrostatic tests, respectively, and 2.0 for thermal transient operations), K_{IM} is the stress intensity factor for pressure loads, and K_{It} is the stress intensity factor that is due to thermal loads (which occur when the vessel is heated up or cooled down). The maximum allowable defect was obtained using $SF = 1$ in all cases. To obtain the stress distributions for pressure loads, a formulation for thick-walled cylinders was used.

The general characteristics of P-T curves are described in the section "P-T Limit Curves;" the specific results for unirradiated steel as well as the influence of neutron embrittlement are introduced in the sections "P-T Curves in the Unirradiated Condition" and "Influence of Irradiation Embrittlement on P-T Curves," respectively. The main features of the analysis to obtain the maximum allowable defect are shown in the section "Maximum Allowable Crack Length."

P-T LIMIT CURVES

A P-T curve represents the maximum allowable pressure P for each value of the temperature T considering the presence of a postulated crack in the vessel. Reciprocally, for a specific P, the P-T curve provides the minimum T to guarantee the structural integrity of the vessel.

As stated in Ref. [5], a flaw with depth a equal to one quarter of the thickness t of the vessel ($a = t/4$, where $t = 177$ mm for this vessel) must be postulated. P-T curves are required to ensure that the vessel operates within the safety margins regarding brittle failure [27]. The previously mentioned combinations of conditions (irradiation level, regulatory scenarios, material description in the DBT region, and crack orientation) were considered in the analysis. In each case, the admissible pressure was obtained as a function of temperature from the failure condition (Eq 10), giving rise to the P-T curves. After obtaining curves corresponding to different combinations of conditions, the most restrictive P-T curve was selected.

P-T Curves in the Unirradiated Condition

Fig. 7a and b shows the P-T curves obtained for (a) the preservice hydrostatic test ($SF = 1.5$) and (b) transient thermal operations. Each shows three P-T curves that correspond to the material responses in the DBT region dictated by the $K_{IR}(T)$ (Eq 1), $K_{Ic}(T)$ (Eq 2), and MC approach (with $P_f = 0.05$). The area under the curves represents the safety region for operation. In all cases, the most restrictive crack was internal and axially oriented. The inherent overconservatism present in the calculations that are based on regulatory procedures is clearly appreciated. In this sense, note that throughout the complete range of temperatures, the admissible pressure obtained by the MC method is substantially higher than that derived after applying the K_{Ic} or K_{IR} curve. On the other hand, as expected, the most conservative material description comes from the K_{IR} curve. In addition, the hydrostatic test is the least demanding loading situation, while the thermal transient operations of the vessel are the most aggressive. Taking into account that, according to the plant specification, the pressure during a hydrostatic test is 10.86 MPa and the operational pressure of the vessel is 7.24 MPa, the minimum required temperatures to guarantee safety against brittle fracture can be determined. Thus, for the hydrostatic test, the minimum temperatures are 56°C, 20°C, and −43°C, depending on whether the K_{IR}, K_{Ic}, or MC models are employed to describe the material response in the DBT region; the equivalent figures for the in-service hydrostatic test would be 39°C, 6°C, and −64°C. This result invites the reflection that ensuring a temperature of 56°C during a hydrostatic test (as deduced in the case of using the K_{IR} curve) may represent a noteworthy logistic drawback. The corresponding minimum temperatures during the entire transient operations should be 78°C, 40°C, and −21°C, respectively. These results highlight the importance of adopting one or the other approach in the management of the structural assessment of a nuclear vessel.

FIG. 7 P-T curves obtained for (a) a preservice hydrostatic test and (b) transient thermal operations, core critical.

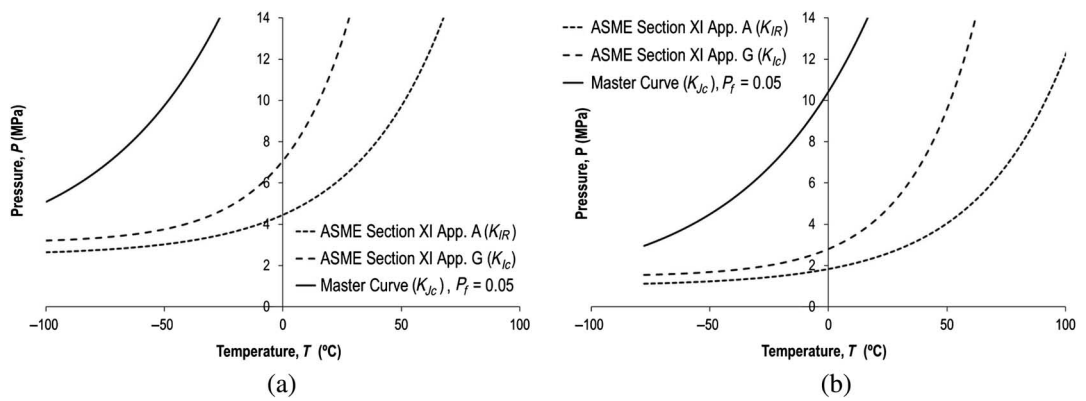

Influence of Irradiation Embrittlement on P-T Curves

Neutron embrittlement implies the reduction of fracture toughness. The approximately 1:1 correlation between $\Delta T_{41\,J}$ and ΔT_0 or ΔRT_{NDT}, as mentioned in the section "The MC" (see Ref. [24]), was considered for obtaining the TTS after irradiation; this information is necessary whether the ASME Code method (curves $K_{Ic}(T)$ and $K_{IR}(T)$ curves) or the MC approach (curve $K_{Jc,Pf=0.05}(T)$) is used. The material condition after 20, 40, and 60 EFPY was determined for structural integrity assessments using the predictions given by "Regulatory Guide 1.99 Rev. 2" [22] and ASTM E900-15e1 [23].

Fig. 8 shows the evolution of the minimum temperature required to avoid brittle fracture as a function of the neutron fluence (expressed in terms of EFPY). The in-service hydrostatic test and thermal transient operations were considered. The most notable conclusions are discussed next:

- In each of the figures, the differences in the level of conservatism derived from the selection of the method to describe the DBT zone are clearly observed. $K_{IR}(T)$ is much more conservative than $K_{Ic}(T)$, which, in turn, is substantially more conservative than the MC approach (with $P_f = 0.05$).
- It is observed that the effect derived from neutron embrittlement (e.g., a shift in transition temperatures) translates to an increase in the minimum temperatures necessary to avoid brittle failure. This change is noticeable for the first years (from 0 to 20 EFPY), but it gradually attenuates over time; this is a well-known feature of neutron embrittlement.
- The results obtained from conventional procedures (K_{IR} and K_{Ic} curves) reveal the drawbacks that could arise when performing the in-service hydrostatic test, since this should be carried out at temperatures of 73°C (K_{IR}) and 40°C (K_{Ic}) after 60 EFPY. However, the predictions derived from the MC method imply that there are no difficulties in the execution of this type of tests (the necessary temperatures are below zero, regardless of the level of irradiation).
- Finally, it is observed that the embrittlement derived from the use of the "Regulatory Guide 1.99 Rev. 2" method is greater than that predicted by ASTM E900. Taking into account that ASTM E900 has been developed more recently, its physical foundations are much more robust, and its predictions are more precise, this result can be interpreted as a new source of overconservatism derived from using "Regulatory Guide 1.99 Rev. 2."

MAXIMUM ALLOWABLE CRACK LENGTH

This type of analysis is focused on determining the maximum allowable crack size for the applied pressure ($P = 10.86$ MPa in the hydrostatic test and $P = 7.24$ MPa for in-service conditions, which include thermal transient operations) and for the state of embrittlement of the material. As in the case of the P-T curves, different combinations of conditions (irradiation level, regulatory scenarios, material description in the DBT region, and crack

FIG. 8 Evolution of the minimum safety temperature to avoid brittle fracture: (a) hydrostatic test ($SF = 1.1$) and (b) thermal transient operations, core critical ($P = 7.24$ MPa in both cases).

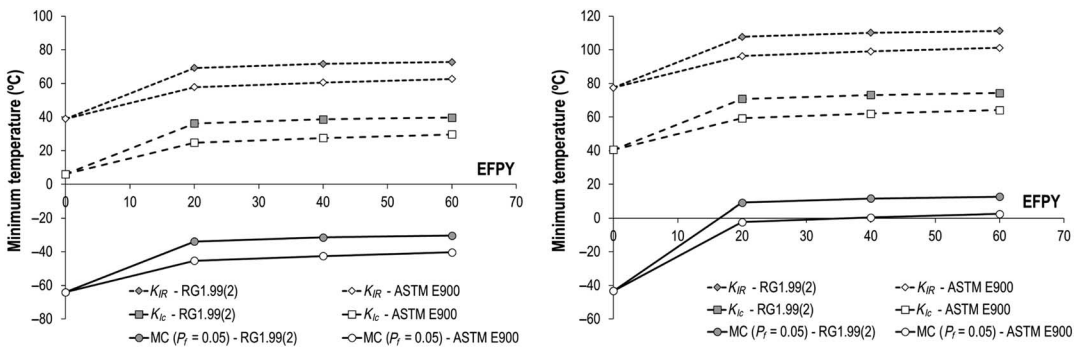

orientation) were considered. The assessment of structural integrity is based on the direct comparison between stress intensity factor and material toughness ($SF = 1$ in Eq 10), which was implemented for the previously mentioned loading conditions (hydrostatic test and thermal transient operations). In addition, two different expressions were considered for the stress intensity factor, namely, the formulations provided by ASME Code Section XI [2] or the FITNET FFS procedure [4]. Only axially oriented cracks were considered, since they are more limiting than circumferentially oriented cracks.

Maximum Allowable Crack Length in the Unirradiated Condition

Table 6 summarizes the values of maximum crack size in the internal and external surfaces of the vessel. In all cases, the hydrostatic test, conducted at room temperature (~25°C), was the limiting scenario. This result contrasts with that obtained in the case of the P-T curves, in which the most restrictive situation corresponded to the thermal transient. This is due to the safety factors adopted in the calculations of the P-T curves, while for the maximum allowable defect, $SF = 1$ was used.

In general, no substantial differences arise between the results obtained for internal (a_{int}) or external (a_{ext}) surface cracks. As in the case of the P-T curves, a marked influence associated with the procedure used to describe the material toughness in the DBT region can be seen. Note that, according to the MC method, admissible cracks range between 45 and 53 % of the thickness of the vessel. In contrast, this range reduces to 22–25 % when using K_{Ic} and 10–12 % when employing K_{IR}. Finally, there is a slight influence associated with the procedure used to define K_I; thus, the formulation proposed by the ASME code leads to results that are slightly more conservative.

Maximum Allowable Crack Length in the Irradiated Condition

For the sake of simplicity, the maximum allowable crack size was determined only after 60 EFPY. Axially oriented cracks were taken into consideration since they are more restrictive. The results are summarized

TABLE 6

Results of the maximum allowable crack length (internal and external surfaces of the vessel) in the unirradiated condition.

K_I Method	Description of Toughness in the DBT Region	a_{int}, mm	Thickness, %	a_{ext}, m	Thickness, %
ASME Code	K_{IR}	17.70	10	17.70	10
	K_{Ic}	38.94	22	40.71	23
	MC ($P_f = 0.05$)	79.65	45	81.42	46
FITNET FFS	K_{IR}	21.24	12	19.47	11
	K_{Ic}	44.25	25	42.48	24
	MC ($P_f = 0.05$)	93.81	53	92.04	52

TABLE 7

Results of the maximum allowable crack length (internal and external surfaces of the vessel) after 60 EFPY. K_I is obtained by means of the ASME Code.

Embrittlement Prediction Model	Description of Toughness in the DBT Region	a_{int}, mm	Thickness, %	a_{ext}, mm	Thickness, %
"RG 1.99 Rev. 2"	K_{IR}	10.62	6	10.62	6
	K_{Ic}	15.93	9	17.70	10
	MC ($P_f = 0.05$)	60.18	34	60.18	34
ASTM E900	K_{IR}	12.39	7	12.39	7
	K_{Ic}	21.24	12	21.24	12
	MC ($P_f = 0.05$)	65.49	37	67.26	38

Note: RG = Regulatory Guide.

TABLE 8

Results of the maximum allowable crack length (internal and external surfaces of the vessel) after 60 EFPY. K_I is obtained by means of the FITNET FFS.

Embrittlement Prediction Model	Description of Toughness in the DBT Region	a_{int}, mm	Thickness, %	a_{ext}, mm	Thickness, %
"RG 1.99 Rev. 2"	K_{IR}	10.62	6	12.39	7
	K_{Ic}	19.47	11	19.47	11
	MC ($P_f = 0.05$)	65.49	37	63.72	36
ASTM E900	K_{IR}	14.16	8	12.39	7
	K_{Ic}	24.78	14	23.01	13
	MC ($P_f = 0.05$)	74.34	42	72.57	41

Note: RG = Regulatory Guide.

in Table 7 using the expression for K_I proposed by the ASME Code and in Table 8 when FITNET FFS was employed. The "Regulatory Guide 1.99 Rev. 2" and ASTM E900 were used to quantify the material embrittlement. In all cases, the loads that are due to hydrostatic tests determine the allowable crack size. This point suggests that a different allowable crack size may be proposed for the hydrostatic test and for operating conditions (thermal transients).

Note that the main reduction in maximum crack size is obtained using the "Regulatory Guide 1.99 Rev. 2" [22] predictive model. Furthermore, in most cases, the maximum allowable crack size is shorter than the postulated flaw ($a = t/4 = 44.25$ mm). In addition, it is observed that the FITNET FFS procedure for K_I is slightly less conservative than the ASME Code.

Summary and Conclusions

Neutron embrittlement is the most significant deterioration mechanism of nuclear vessel steels. The reduction undergone by the toughness of the material over the exposure time may influence the viability of the plant and lead to its closure. This phenomenon is of particular relevance when steel operates at a temperature within the DBT region. For this reason, NPPs monitor the evolution of steel properties through so-called surveillance programs, in particular the toughness in the transition region. In spite of this, it is now possible to estimate the embrittlement of the steel using correlations elaborated from experimental and theoretical considerations.

Broadly speaking, two large families of methods are available to assess the structural integrity of a nuclear vessel. First, according to the current legislation, the initial toughness of the steel in the DBT region is described in a deterministic way by means of the initial (unirradiated material) reference temperature $RT_{NDT(U)}$ and its shift over time, ΔRT_{NDT}. It is considered that ΔRT_{NDT} can be obtained experimentally from the results derived from the Charpy impact test so that $\Delta RT_{NDT} = \Delta T_{41\ J}$. However, in the absence of experimental data, "Regulatory Guide 1.99 Rev. 2" allows ΔRT_{NDT} to be estimated from the chemical composition of the steel and the neutron fluence. There is a more recent alternative approach based on the description of the behavior of the material in the transition region through the so-called MC, which offers a probabilistic description of the brittle fracture of the material. The reference temperature T_0 is the material property that defines the MC, which is obtained from K_{Jc} fracture toughness tests. In addition, embrittlement can be estimated by means of the procedure of ASTM E900, which takes into account the chemical composition of the material and the neutron fluence while also considering the neutron flux and irradiation temperature.

In this research, an exhaustive study on the performance of the steel (carbon steel grade SA-508M Grade 3 Class 1) of a vessel currently under construction was carried out. The work includes a complete experimental characterization of the material that serves as a basis for the assessment of structural integrity. The main conclusions are summarized as follows:

- The characterization comprises the following methods: chemical composition, tension tests (as a function of temperature), Charpy impact tests (as a function of temperature), Pellini DW tests, and K_{Jc} fracture toughness tests (to determine the reference temperature T_0).
- The high isotropy shown by the material can be highlighted as the most significant result. Thus, the tensile responses in the L and T orientations are virtually identical. This outcome was also observed after comparing the Charpy or fracture toughness tests in the LT and TL orientations, in which TL orientation appears to be slightly weaker (the differences in transition temperatures $T_{27\ \mathrm{J}}$, $T_{41\ \mathrm{J}}$, and $T_{68\ \mathrm{J}}$ are between 8.6°C and 12.5°C, and the difference of T_0 amounts to 6°C). In general, the process of forming the steel during the manufacture of the vessel induces microstructural changes that produce the anisotropic behavior of the material [12]. In this sense, the strength in the T direction is considered to be lower than in the L direction, and the toughness in the TL orientation is in most cases lower than that in the LT orientation. These experimental results denote, therefore, a careful manufacturing process designed to optimize the strength of the material.
- The assessment of structural integrity was carried out from two complementary approaches. On the one hand, the P-T curves were obtained both in the unirradiated condition and for different levels of irradiation: 20, 40, and 60 EFPY. On the other hand, a catalog of maximum admissible defect has been obtained in the same scenarios.
- The most notable outcome consists of the inherent overconservatism present in the calculations based on regulatory procedures. The results of the P-T curves or the size of the admissible defect strongly depend on the procedure used to describe the material behavior in the transition region. Thus, when the K_{Ic} or K_{IR} curves are used, a much more conservative picture is obtained than when using the MC method.
- Two different scenarios were compared by means of the P-T curves: hydrostatic test and thermal transient conditions (including heating-up and cooling-down operations). The assessment proves that the hydrostatic test is the least demanding loading situation, while the thermal transient operations of the vessel are the most aggressive for plant operation conditions.
- The conservatism associated with the methodology of analysis may compromise the viability of the plant. Thus, the minimum temperature required to perform a hydrostatic test is 56°C, 20°C, and −43°C when the K_{IR}, K_{Ic}, and MC models are employed, respectively. This result is even more severe in the irradiated condition; thus, the hydrostatic test should be carried out at temperatures above 80°C (K_{IR}) or 40°C (K_{Ic}) after 60 EFPY. In contrast, the minimum temperature that arises after employing the MC method is below zero in all cases.
- The maximum size of admissible defect is also affected by the procedure that is used to characterize the DBT region. In this sense, the admissible cracks range between 45 % and 53 % of the thickness of the vessel when using the MC. In contrast, this range reduces to 22–25 % when using K_{Ic} and 10–12 % when employing K_{IR}.

Regulatory authorities in some countries have already incorporated the MC procedure as an available tool for surveillance programs and for the assessment of the structural integrity of nuclear vessels. The conclusions reached in this study show that the methods traditionally used for the description of fracture toughness in the DBT region suffer from intrinsic limitations that encourage the modification of the regulations to fully incorporate the MC approach.

ACKNOWLEDGMENTS

This article describes the work performed by the Laboratory of Science and Engineering of Materials of the University of Cantabria and the Technological Center of Components. This project was carried out with the financial support of Sociedad para el Desarrollo Regional de Cantabria (SODERCAN) and Equipos Nucleares S.A. (ENSA), to whom the authors would like to express their gratitude.

References

[1] American Society of Mechanical Engineers, "BPVC Section III-Rules for Construction of Nuclear Facility Components," *Boiler and Pressure Vessel Code*, American Society of Mechanical Engineers, New York, NY, 2017, pp. 1–501.

[2] American Society of Mechanical Engineers, "BPVC Section XI-Rules for Inservice Inspection of Nuclear Power Plant Components," *Boiler and Pressure Vessel Code*, American Society of Mechanical Engineers, New York, NY, 2017, pp. 1–731.
[3] ASTM E1921-17a, *Standard Test Method for Determination of Reference Temperature, T_0, for Ferritic Steels in the Transition Range* (Superseded), ASTM International, West Conshohocken, PA, 2017, www.astm.org
[4] Hadley, I., "Overview of the European Fitnet Fitness-for-Service Procedure (June 2008)," TWI Ltd., Cambridge, UK, http://web.archive.org/web/20181217145443/https://www.twi-global.com/technical-knowledge/published-papers/overview-of-the-european-fitnet-fitness-for-service-procedure-june-2008 (accessed 17 Dec. 2018).
[5] United States Nuclear Regulatory Commission, "50.61 Fracture Toughness Requirements for Protection against Pressurized Thermal Shock Events," *NRC Regulations Title 10, Code of Federal Regulations*, United States Nuclear Regulatory Commission, Washington, DC, 2011, https://web.archive.org/web/20181213165008/https://www.nrc.gov/reading-rm/doc-collections/cfr/part050/part050-0061.html (accessed 13 Dec. 2018).
[6] Wallin, K., Saario, T., and Törrönen, K., "Statistical Model for Carbide Induced Brittle Fracture in Steel," *Met. Sci.*, Vol. 18, No. 1, 1984, pp. 13–16, https://doi.org/10.1179/030634584790420384
[7] Wallin, K., "The Scatter in K_{IC}-Results," *Eng. Fract Mech*, Vol. 19, No. 6, 1984, pp. 1085–1093, https://doi.org/10.1016/0013-7944(84)90153-X
[8] Wallin, K., "The Size Effect in K_{IC} Results," *Eng Fract Mech*, Vol. 22, No. 1, 1985, pp. 149–163, https://doi.org/10.1016/0013-7944(85)90167-5
[9] Wallin, K., "A Simple Theoretical Charpy V - KIc Correlation for Irradiation Embrittlement," *Innovative Approaches to Irradiation Damage and Fracture Analysis*, American Society of Mechanical Engineers, New York, NY, 1989, pp. 93–100.
[10] Merkle, J. G., Wallin, K., and McCabe, D. E., *Technical Basis for an ASTM Standard on Determining the Reference Temperature, T_0, for Ferritic Steels in the Transition Range*, United States Nuclear Regulatory Commission, Washington, DC, 1998, pp. 1–149.
[11] Ferreño, D., Lacalle, R., Cicero, R., Scibetta, M., Gorrochategui, I., van Walle, E., and Gutiérrez-Solana, F., "Structural Integrity Assessment of a Nuclear Vessel with FITNET FFS and Master Curve Approach," *Eng Fail Anal*, Vol. 17, No. 1, 2010, pp. 259–269, https://doi.org/10.1016/j.engfailanal.2009.06.007
[12] Ferreño, D., Scibetta, M., Gorrochategui, I., Lacalle, R., van Walle, E., and Gutiérrez-Solana, F., "Validation and Application of the Master Curve and Reconstitution Techniques to a Spanish Nuclear Vessel," *Eng Fract Mech*, Vol. 76, No. 16, 2009, pp. 2495–2511, https://doi.org/10.1016/j.engfracmech.2009.08.010
[13] Ferreño, D., Lacalle, R., Gorrochategui, I., and Gutiérrez-Solana, F., "Fracture Characterisation of a Nuclear Vessel Steel under Dynamic Conditions in the Transition Region," *Eng Fail Anal*, Vol. 17, No. 2, 2010, pp. 464–472, https://doi.org/10.1016/j.engfailanal.2009.09.001
[14] Ferreño, D., Lacalle, R., Gorrochategui, I., and Gutiérrez-Solana, F., "Analysis of Dynamic Conditions during Thermal Transient Events for the Structural Assessment of a Nuclear Vessel," *Eng Fail Anal*, Vol. 17, No. 4, 2010, pp. 894–905, https://doi.org/10.1016/j.engfailanal.2009.10.024
[15] Scibetta, M., Ferreño, D., Gorrochategui, I., Lacalle, R., van Walle, E., Martín, J., and Gutiérrez-Solana, F., "Characterisation of the Fracture Properties in the Ductile to Brittle Transition Region of the Weld Material of a Reactor Pressure Vessel," *J Nucl Mater*, Vol. 411, No. 1, 2011, pp. 25–40, https://doi.org/10.1016/j.jnucmat.2011.01.024
[16] Heerens, J. and Hellmann, D., "Application of the Master Curve Method and the Engineering Lower Bound Toughness Method to Laser Welded Steel," *J Test Eval*, Vol. 31, No. 3, 2003, pp. 215–221, https://doi.org/10.1520/JTE12419J
[17] ASTM E399-12e3, *Standard Test Method for Linear-Elastic Plane-Strain Fracture Toughness KIc of Metallic Materials* (Superseded), ASTM International, West Conshohocken, PA, 2012, www.astm.org
[18] ASTM E1820-17, *Standard Test Method for Measurement of Fracture Toughness* (Superseded), ASTM International, West Conshohocken, PA, 2017, www.astm.org
[19] Wallin, K., "Effect of Strain Rate on the Fracture Toughness Reference Temperature T_0 for Ferritic Steels," presented at the *1997 TMS Annual Meeting*, Orlando, FL, Feb. 9–13, 1997, The Minerals, Metals & Materials Society, Pittsburgh, PA, pp. 171–182.
[20] Joyce, J., Tregoning, R., and Roe, C., "On Setting Testing Rate Limitations for the Master Curve Reference Temperature, To, of ASTM E 1921," *J Test Eval*, Vol. 34, No. 2, 2006, pp. 121–127, https://doi.org/10.1520/JTE14108
[21] Hernández, R., Romero, J., Vázquez, S., Santillán, M., and Scibetta, M., "Loading Rate Effect on the Master Curve Reference Temperature, T_0, for the A533 B Material," *J Test Eval*, Vol. 38, No. 2, 2010, pp. 195–202, https://doi.org/10.1520/JTE102438
[22] United States Nuclear Regulatory Commission, "Regulatory Guide 1.99: Radiation Embrittlement of Reactor Vessel Materials, Revision 2," United States Nuclear Regulatory Commission, Washington, DC, 1988, pp. 1–10.
[23] ASTM E900-15e1, *Standard Guide for Predicting Radiation-Induced Transition Temperature Shift in Reactor Vessel Materials*, ASTM International, West Conshohocken, PA, 2015, www.astm.org
[24] Sokolov, M. A. and Nanstad, R. K., "Comparison of Irradiation-Induced Shifts of K_{Jc} and Charpy Impact Toughness for Reactor Pressure Vessel Steels," *Effects of Radiation on Materials: 18th International Symposium, ASTM STP1325*, R. K. Nanstad, M. L. Hamilton, F. A. Garner, and A. E. Kumar, Eds., ASTM International, West Conshohocken, PA, 1999, pp. 167–190, https://doi.org/10.1520/STP13863S
[25] American Society of Mechanical Engineers, "BPVC Section II-Materials-Part A-Ferrous Materials Specifications," *Boiler and Pressure Vessel Code 2017*, American Society of Mechanical Engineers, New York, NY, 2017, pp. 1–813.

[26] ASTM E185-16, *Standard Practice for Design of Surveillance Programs for Light-Water Moderated Nuclear Power Reactor Vessels*, West Conshohocken, PA, ASTM International, 2016, www.astm.org
[27] ASTM E8/E8M-16a, *Standard Test Methods for Tension Testing of Metallic Materials*, ASTM International, West Conshohocken, PA, 2016, www.astm.org
[28] ASTM E23-16b, *Standard Test Methods for Notched Bar Impact Testing of Metallic Materials*, ASTM International, West Conshohocken, PA, 2016, www.astm.org
[29] ASTM E208-06(2012), *Standard Test Method for Conducting Drop-Weight Test to Determine Nil-Ductility Transition Temperature of Ferritic Steels* (Superseded), ASTM International, West Conshohocken, PA, 2012, www.astm.org